Available online at www.sciencedirect.com

ScienceDirect

Physics Procedia 66 (2015) 576 – 585

Physics Procedia

C 23rd Conference on Application of Accelerators in Research and Industry, CAARI 2014

Mechanical Properties of Metal Nitrides for Radiation Resistant Coating Applications: A DFT Study

Oscar U. Ojeda Mota[a], Roy A. Araujo[b], Haiyan Wang[b], Tahir Çağın[a,c]

[a]*Laboratory of Computational Engineering of Nanomaterials, Artie McFerrin Department of Chemical Engineering, Texas A&M University, College Station, TX, 77843-3122, USA*

[b]*Department of Electrical and Computer Engineering, Texas A&M University, College Station, TX 77843-3128, USA*

[c] *Department of Materials Science and Engineering, Texas A&M University, College Station, TX, 77843-3003, USA*

Abstract

Metal nitrides compounds like aluminum nitride (AlN), titanium nitride (TiN), tantalum nitride (TaN), hafnium nitride (HfN) and zirconium nitride (ZrN) are of great interesting because of their chemical and physical properties such as: high melting point, resistivity, thermal conductivity and extremely high hardness. They are the materials of choice for various applications like protective coating for tools, diffusion barriers or metal gate contact in microelectronics, and lately their potential applications as radiation-resistive shields. In order to assess their use for radiation tolerance we have studied the structural, mechanical and electronic properties. We have evaluated the anisotropic elastic constants and their pressure dependence for three different crystalline phases: B1-NaCl, B2-CsCl, and B3-ZnS crystal structures. In addition to these cubic polymorphs, we also have studied potential hexagonal structures of some of the same metal nitrides. All computations are carried out using first principles Density Functional Theory (DFT) approach.

Selection and peer-review under responsibility of the Organizing Committee of CAARI 2014

Keywords: nitrides; phase stability; polymorphism; elasticity; ab initio; DFT; equation of state

* Corresponding author. Fax: 979-862-6835

E-mail address: tcagin@tamu.edu

Selection and peer-review under responsibility of the Organizing Committee of CAARI 2014

doi:10.1016/j.phpro.2015.05.077

1. Introduction

Because of their chemical and physical properties such as: high melting point, resistivity, thermal conductivity and extremely high hardness, IIIA group binary nitride compounds are commonly regarded as wide band-gap semiconductors (Song et al., 2006) with important technological use (Bazhanov et al., 2005, 2004; Chen et al., 2005; Ching & Harmon, 1986; Figueroa et al., 2004; Kang et al., 2003; Lambrecht et al., 2005; Lopez & Staia, 2005; Pierson, 1996; Stampfl et al., 2001; Stejskal & Leitner, 2002; Storms, 1964; Terao, 1971; Wu et al., 2005). As semiconductor devices pushes the scale and size limit, the study of the different phases (Conroy & Christensen, 1977; Gerstenberg & Calbick, 1964; Petrunin & Sorokin, 1982; Terao, 1971) and mechanical properties (Mehl,1993; Rivadulla et al., 2009) become of particular relevance, particularly in the case of interphases and highly strained states that can be found by multilayer stacking (Edelstein1997). There is also increased interest in the use of these materials as structural ceramics due to being chemical and radiation inert (Ferreira da Silva et al., 2005; Gusev, 1997; Hu et al., 2002; Levy et al., 1999; M. Lerch, 1996; Werner H. Baur, 1996; Zaoui, 2003), and the high energy of formation required to create defects in them (Christensen, 1994). Systems like some aluminum nitrides and oxinitrides are of interest due to their optical properties, which constitute them as transparent mechanical barriers (Clayton, 2011).

These nitrides display a large number of stable crystal structures and polymorphic phase transitions under pressure. In the case of zirconium nitride ZrN, the most stable phase is the cubic (B1) “rocksalt” structure (Wycko1963). The existence of this particular structure at ambient conditions is rare amongst binary metal nitrides; for AlN and other aluminum carbonitrides (Jerey & Wu, 1963) display wurzite or “B4” structure. Although some experimental reports have suggested the existence of a metastable (Meng, 1994) zincblende phase (B3), the relative energetic or mechanical stability of these two phases is still not clear. For TaN at ambient conditions the crystal structure has P-62m symmetry, which is known as “θ” phase. The structure known as “ε-hex” undergoes a phase transformation at high temperature and pressure to the θ-phase (Tsvyashchenko et al., 1980). Other structures include; “NaCl” structure observed at high pressures, as well as the “CsCl” structure, which is observed in films electrochemically deposited on template substrates (Georg Brauer & Karl Heinz Zapp, 1954; Mashimo et al., 1997) have been reported. The tetragonal structure has been deemed as the most stable one (Zerr et al., 2009). For instance, Hf_3N_4 compound may have interesting optical and magnetic properties (Zerr et al., 2003). Given the diversity of reported phases, a complete understanding of the energetics and mechanical properties is needed in order to clarify their relative stability. Many applications of these materials require improved performance at extreme pressure, hence a better understanding their behavior at high pressures is of paramount importance.

Results obtained from density functional theory (DFT) level of theory (Hohenberg & Kohn, 1964; Kohn & Sham, 1965) calculations on the binary nitrides of aluminum, titanium, zirconium, tantalum and hafnium (AlN, TiN, ZrN, TaN and HfN) are reported in the present study. As compared to previous studies (Ching & Harmon, 1986; Merad et al., 2003; Wright, 1995), full structure optimizations (e.g. ionic positions, c/a ratios) are performed for structures.

2. Methods

In these calculations, projector augmented wave type of potentials (Kresse & Joubert, 1999) (PAW) with Perdew-Berke-Ernzerhof exchange correlation functionals were employed with the intention of obtaining energy-volume and energy pressure characteristics at the optimized (relaxed) structural parameters (e.g. c/a ratio). Either the conjugate-gradient iterative scheme or the block Davidson method for the Kohn-Sham matrix diagonalization as implemented in VASP (Kresse & Furthmuller, 1996a,b; Kresse & Hafner, 1993) is used. A Monkhost-Pack mesh grid for the case of cubic structures, and a Γ-centered mesh for hexagonal structures were employed for the calculations. The convergence criterion for each system is kept to less than 4 meV/atom independent from the size of the unit cells used. The method of Methfessel-Paxton (MP) of different order is used for smearing of the occupation near the Fermi surface, with a width of 0.1 eV. The tetrahedron method with Blöch corrections is used in accurate calculation of density of states and electronic band structure. When hard PAW potentials are not used, convergence is found for an accuracy value smaller than 0.5 meV per unit cell. Some DFT studies that involved the study of binary nitrides system under different pressures via plane wave pseudopotentials results are performed with experimentally observed pressure c/a ratios (Ching & Harmon, 1986; Merad et al., 2003; Wright, 1995). Others have

used FLAPW method or the linear muffin-tin-orbital (LMTO) method (Christensen, 1994), and linearized augmented plane-waves (Bazhanov et al., 2005) (LAPAW) with the generalized gradient approximation (GGA) method (Sedmidubsky & Leitner, 2006). Some other theoretical studies make use of pseudopotentials or semi-empirical methods within the LDA approximation, which also observe a smaller band gap for similar systems (Pugh et al., 1999). Calculations of the total energy have been performed from unit cells obtained by changing the volume of the crystalline phases.

Elastic stiffness coefficients can be obtained from the expansion of the crystal potential from the reference state, "Φ_0", at a reference volume "V0" in terms of an applied strain (Hill, 1975;Wallace, 1972);

$$\Phi = \Phi_0 + V_0\sigma_{ij}\varepsilon_{ij} + \frac{V_0}{2}C_{ijkl}\varepsilon_{ij}\varepsilon_{kl} + \frac{V_0}{6}C_{ijklmn}\varepsilon_{ij}\varepsilon_{kl}\varepsilon_{mn} + ... \quad (0.1)$$

Assuming relaxed state, and through Voigt's notation (Nye, 1985) the fourth rank-tensor "C_{ijkl}" is now the second order elastic stiffness tensor:

$$C_{ij} = \frac{1}{V_0}\frac{\delta^2\Phi}{\delta\in_i \delta\in_j} \quad (0.2)$$

A strain size close to the equilibrium parameters is found, so that energy differences are larger compared to the intrinsic error arising from the self-consistent calculation itself. Strain values employed ranged from 0.005 to 0.08. To elucidate the energetics of the different studied phases, a lattice expansion is performed from the relaxed zero-stress structure. The Energy-Volume results are then fitted to a fourth order Birch-Murnaghan (Birch, 1947) equation of state (Ojeda Mota & Cagın, 2011) based on finite elastic theory and a power series expansion of the free energy.

$$P/B_0 = 3f(1+2f)^{\frac{5}{2}}\left[1-\frac{1}{2}\left(\frac{\delta_3}{\delta_2}\right)f+\frac{1}{6}\left(\frac{\delta_4}{\delta_2}\right)f^2....\right] \quad (0.3)$$

Here:

$$V/V_0 = (1+2f)^{-\frac{3}{2}} \quad (0.4)$$

And:

$$\frac{\delta_3}{\delta_2} = 12 - 3B'_0 \quad (0.5)$$

$$\frac{\delta_4}{\delta_2} = 9B_0B''_0 + 9(B_0)^2 - 63B'_0 + 143 \quad (0.6)$$

This approach accurately represents the equilibrium parameters when a large range of thermodynamic data along a given isotherm is available. The minimum energy (E_0), equilibrium volume (V_0), bulk modulus (B_0) and the first

derivative of the bulk modulus (B'0) are thus obtained

3. Results

3.1. Equations of states (EoS), parameters associated with EoS and physical properties of different polymorphs

We present the pressure vs. volume behavior of TaN, TiN, ZrN HfN and AlN (Figure 1). The equilibrium volume for each of the crystalline phases corresponds at a minimum point of their respective E-V curve (Figure 2). Corresponding pressures in Figure 1 are determined from internal stress tensor and confirmed from each point on the E vs. V Equation of State curves in Figure 2; indicating good convergence with respect to the calculation parameters. We have included calculations for other phases yet to be reported to form basis for future reference. For example, we include in the AlN system, two phases, the β-tin and B2 structures. These, as well as the two structures B35, orthogonal and Th_3P_4 phases are included in our studies for binary metal nitrides, though they have never been observed experimentally. Equilibrium volumes, found at the intersection of the value at P=0, compare with the values obtained form the fourth order BM EOS, as expected. We have included the equilibrium parameters for each system.

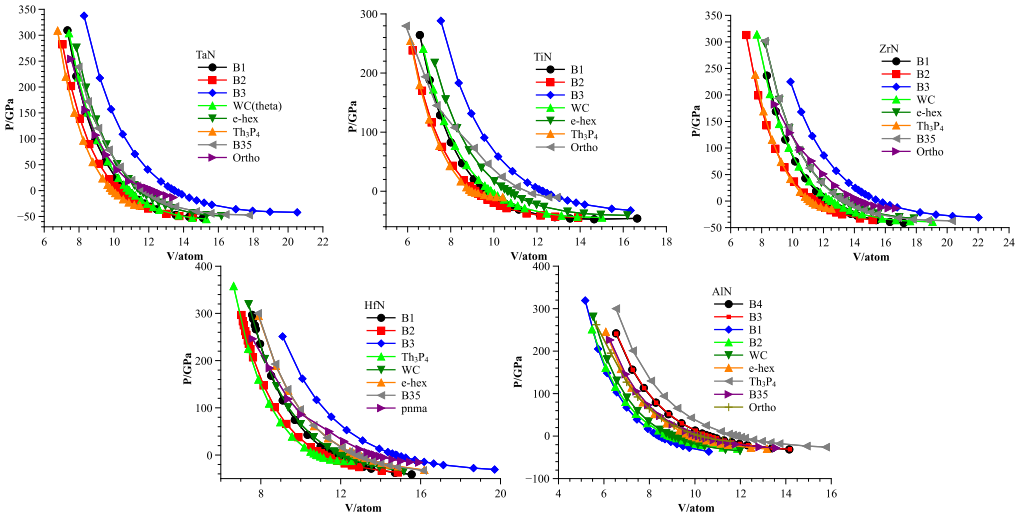

Figure 1. Pressure behavior of the different phases studied here.

For AlN, the tetrahedrally coordinated Al atom is surrounded by four holes in a regular N tetrahedron in the wurtzite structure. The characteristic structural parameter u deviates from the ideal 1.633 ratio with a value of 1.603, ascribing this higher ionic character, as compared to other wurtzite systems (Schulz & Thiemann 1977). From earlier calculations using orthogonalized linear combination of atomic orbitals approximation (OLCAO) a band gap of 4.64 eV was reported. In its wurzite structure, AlN has an energy band gap of 6.02 eV.

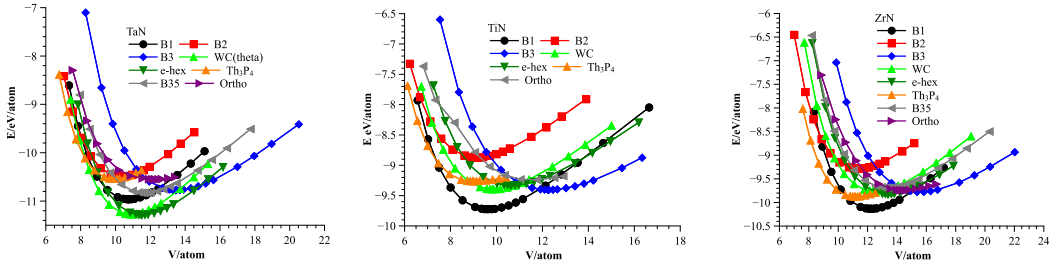

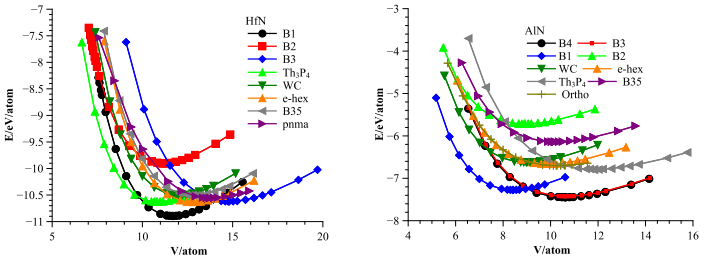

Figure 2. Energetic behaviour of the different phases studied here

Through the 4th order Birch-Murnaghan EoS enable us to determine the equilibrium structural parameters and isotropic mechanical properties for each crystal structure. We summarize our results in the following Tables 1-5.

Table 1. Equilibrium properties for the systems TaN

Phase	B_0	B'_0	B''_0	V_0/atom	E_0/atom	A	C/A	B/A
B1	345.69	4.60	-2.99	10.76	-10.96	4.4145		
B2	322.86	4.40	-2.65	10.33	-10.4903	2.7441		
B3	255.34	4.31	-3.48	14.84	-10.7712	4.7613		
Th_3P_4	326.58	4.99	-3.91	9.93	-10.5422	6.5262		
B35	284.03	4.23	-2.95	11.67	-10.8326	5.2608	0.5555	
e-hex	318.70	4.49	-3.29	11.51	-11.2851	5.2135	0.5628	
WC	351.83	4.45	-2.92	10.89	-11.2722	2.9468	0.9827	
ortho	209.89	2.83	-1.51	12.28	-10.5513	9.1077	1.3468	0.3379

Table 2. Equilibrium properties for the systems TiN

Phase	B_0	B'_0	B''_0	V_0/atom	E_0/atom	A	C/A	B/A
B1	293.68	4.54	-3.09	9.63	-9.7221	4.2552		
B2	268.05	4.42	-3.05	9.14	-8.8686	2.6342		
B3	210.39	4.34	-3.91	12.28	-9.4020	4.6134		
Th_3P_4	179.51	6.84	-17.35	9.23	-9.2700	6.3057		
e-hex	250.40	4.30	-3.14	10.65	-9.3327	5.1305	0.5462	
WC	270.50	4.30	-2.91	9.92	-9.3947	2.9074	0.9268	
B35	229.25	4.32	-3.33	10.61	-9.1346	5.0640	0.5658	
ortho	89.23	7.53	-52.16	11.49	-9.2425	9.3047	0.3442	1.1602

Table 3. Equilibrium properties for the systems ZrN

Phase	B_0	B'_0	B''_0	V_0/atom	E_0/atom	A	C/A	B/A
B1	265.66	4.65	-4.08	12.24	-10.13	4.6080		
B2	233.37	4.25	-3.37	11.40	-9.2863	2.8366		
B3	198.73	3.77	-3.21	15.59	-9.7762	4.8744		
Th_3P_4	227.39	5.68	-12.45	11.20	-9.8753	6.7808		
B35	226.38	4.35	-4.05	13.35	-9.6862	5.4365	0.5756	
e-hex	221.23	4.41	-4.33	13.41	-9.8198	5.5099	0.5553	
WC	236.14	4.34	-3.87	12.52	-9.7641	3.1463	0.9280	
pnma	179.89	2.37	-3.10	14.41	-9.7404	10.0575	0.3440	1.1531

Table 4. Equilibrium properties for the systems HfN

Phase	B_0	B'_0	B''_0	V_0/atom	E_0/atom	A	C/A	B/A
B1	279.60	4.41	-3.16	11.69	-10.8939	4.5390		
B2	230.34	3.81	-2.30	11.16	-9.8853	2.8163		
B3	164.54	4.16	-4.11	14.80	-10.6250	4.9105		
Th_3P_4	207.08	5.67	-9.16	10.81	-10.6257	6.7143		
e-hex	224.70	4.10	-3.15	12.86	-63.7939	5.4162	0.5601	
WC	241.23	4.14	-2.93	12.04	-10.5003	3.0966	0.9361	
B35	231.20	4.06	-2.98	12.81	-10.5041	5.3704	0.5723	
ortho	171.38	4.68	-13.22	13.76	-10.5538	9.9036	1.1533	0.3438

Table 5. Equilibrium properties for the systems AlN

Phase	B_0	B'_0	B''_0	V_0/atom	E_0/atom	A	C/A	B/A
B1	249.24	4.08	-2.90	8.43	-7.27	4.0690		
B2	187.79	4.21	-4.07	8.92	-5.7157	2.6133		
B3	191.00	-3.61	3.99	10.66	-7.4219	4.4010		
Th_3P_4	159.56	3.95	-4.19	11.84	-6.7678	6.9208		
B4	192.51	3.94	-3.47	10.63	-7.4449	3.1286	1.6033	
B35	175.27	4.05	-4.00	10.21	-6.1372	5.0717	0.5416	
e-hex	189.28	4.05	-3.71	9.92	-6.6606	5.0218	0.5415	
WC	216.40	4.06	-3.19	9.01	-6.6200	2.8373	0.9100	
ortho	185.92	2.71	-2.04	10.27	-6.7057	8.9593	1.1869	0.3367

3.2. Second order elastic constants of TaN, TiN, ZrN, HfN and AlN polymorphs

In order to better understand the phase stability and anisotropic mechanical properties of these binary nitrides, we have evaluated the independent elastic stiffness coefficients of different metal nitrides in different crystal phases. These anisotropic second order elastic constants and bulk moduli are tabulated in the following tables, from Table 6 through Table 10, for TaN, TiN, ZrN, HfN and AlN, respectively.

Table 6. Mechanical properties for the system: TaN

	B1	**B2**	**B3**	**Th_3P_4**	**B35**	**WC**	**e-hex**
C_{11}	706.97	930.24	303.36	564.96	395.37	641.02	539.15
C_{12}	155.70	19.71	233.55	244.81	210.36	214.60	220.38
C_{33}	-	-	-	-	766.74	822.20	678.16
C_{44}	208.20	104.96	26.78	181.88	272.39	262.71	273.12
C_{13}	-	-	-	-	225.52	196.43	192.39
B_0	339.46	323.22	256.82	351.53	320.03	368.79	329.64

pnma						
C_{11}	**C_{22}**	**C_{33}**	**C_{12}**	**C_{13}**	**C_{23}**	**C_{44}**
395.90	249.16	369.40	142.41	130.83	56.38	21.08
		C_{66}	**C_{55}**	**B_0**		
		91.49	127.86	185.96		

Table 7. Mechanical properties for the system: TiN

	Exp	**B1**	**B2**	**B3**	**Th_3P_4**	**WC**	**e-hex**	**B35**
C_{11}	625	596.79	597.6174	305.74	363.54	482.65	339.30	338.23
C_{12}	165	112.19	110.72	174.68	100.72	182.25	246.85	141.52
C_{33}	-	-	-	-	-	761.57	521.41	644.45
C_{44}	163,168*	153.68	29.81	84	124.99	113.07	125.10	196.86
C_{13}	-	-	-	-	-	119.17	124.30	178.47
B_0	318	273.72	273.02	218.37	188.33	285.34	243.43	257.53

pnma							
C_{11}	**C_{22}**	**C_{33}**	**C_{12}**	**C_{13}**	**C_{23}**	**C_{44}**	**C_{55}**
345.06	352.16	265.50	129.56	114.89	112.94	77.17	12.77
			C_{66}	**B_0**			
			76.66	186.39			

Table 8. Mechanical properties for the system: ZrN

	Exp	B1	B2	B3	Th_3P_4	B35	WC	e-hex
C_{11}	471	591.36	458.32	448.86	450.08	310.75	414.90	311.00
C_{12}	88	101.13	113.05	84.81	134.27	121.22	158.45	199.17
C_{33}	-	-	-	-	-	599.36	620.80	465.08
C_{44}	138	104.61	45.76	92.50	157.90	201.08	80.14	137.90
C_{13}	-	-	-	-	-	148.12	105.68	128.07
B_0	215.67	264.54	228.14	206.16	239.54	228.42	243.36	221.96

pnma							
C_{11}	C_{22}	C_{33}	C_{12}	C_{13}	C_{23}	C_{44}	C_{55}
338.62	306.31	242.26	129.00	110.64	95.46	7.18	-5.14
			C_{66}	B_0			
			78.98	173.04			

Table 9. Mechanical properties for the system: HfN

	Exp	B1	B2	B3	Th_3P_4	WC	e-hex	B35
C_{11}	679	525.75	508.01	251.86	439.21	461.13	301.89	346.22
C_{12}	119	142.63	98.16	166.34	101.15	140.25	227.96	108.46
C_{33}	-	-	-	-	-	649.43	476.68	653.87
C_{44}	150	223.12	14.79	109.91	146.74	94.28	155.94	208.75
C_{13}	-	-	-	-	-	105.55	128.69	148.01
B_0	305.67	270.34	234.78	194.85	213.84	252.71	227.91	239.47

pnma							
C_{11}	C_{22}	C_{33}	C_{12}	C_{13}	C_{23}	C_{44}	C_{55}
366.50	331.61	264.69	137.09	106.67	102.35	68.91	64.57
			C_{66}	B_0			
			91.31	183.89			

Table 10. Mechanical properties for the system: AlN

	Exp	B1	B2	B3	Th_3P_4	B4	B35	WC	e-hex
C_{11}	410,345	426.02	559.27	280.75	263.34	377.84	81.93	528.75	480.17
C_{12}	125,149	163.68	4.68	153.38	95.45	127.05	325.92	140.91	143.74
C_{33}	388.5,395	-	-	-	-	355.57	602.64	941.98	601.36
C_{44}	127,118	205.07	-136.19	117.59	56.24	163.16	80.86	-66.29	-60.94
C_{13}	98.9,120	-	-	-	-	118.63	21.00	-42.02	-1.26
B_0	228/202	251.13	189.54	195.84	151.41	204.43	166.93	234.80	204.90

pnma								
C_{11}	C_{22}	C_{33}	C_{12}	C_{13}	C_{23}	C_{44}	C_{55}	C_{66}
269.14	339.79	141.73	152.91	112.16	107.23	64.61	14.30	85.81
				B_0				
				166.14				

3.3. Phase Stability

In order to assess the phase stability ranges of different polymorphs and potential pressure induced phase transitions between these phases, we have used the Equation of State (E vs. V (lattice parameters)) and associated calculated pressures at each volume (lattice parameters) to determine the 0 K enthalpy from the aforementioned DFT computations for each of Metal nitrides, since the conducted the most relevant information can be extracted from the Enthalpy-Pressure relationships. The variation of enthalpy as a function of "applied pressures" on the crystal

structures is displayed (Figure 3) for TaN, TiN, ZrN, HfN and AlN, respectively, in the crystal phases we considered in this study.

For TiN, a transition from the crystal structure B1 (NaCl) to B2 (CsCl) occurs at approximately 3458 kbar (compressive). From the enthalpy-pressure figure, the most stable phase at a zero pressure is the B1 (NaCl) crystal phase as compared to the B2 (CsCl) and B3 (ZnS) crystalline structures. Similar results observed for HfN. The phase transitions are in close resemblance to the behavior observed for TiN, B1- B2 at 280 GPa, with the stable phase at zero pressure being B1 with a volume of 23.38 3 or 4.53 of lattice parameter.

For TaN, from the enthalpy-pressure curves we determine the most stable phase at zero pressure as the δ-hexagonal phase. Two transitions can be seen; TaN-ε-hex and WC, which practically coexist at 0K, with ε-hex being more favorable. The other one occurs from δ-hexagonal (theta or WC) to the B2 at pressures of 235.0 GPa. The equilibrium structure is observed at a volume of 21.66 3 or with lattice parameters a = 2.94 and c = 2.89 at zero pressure for the hexagonal phase.

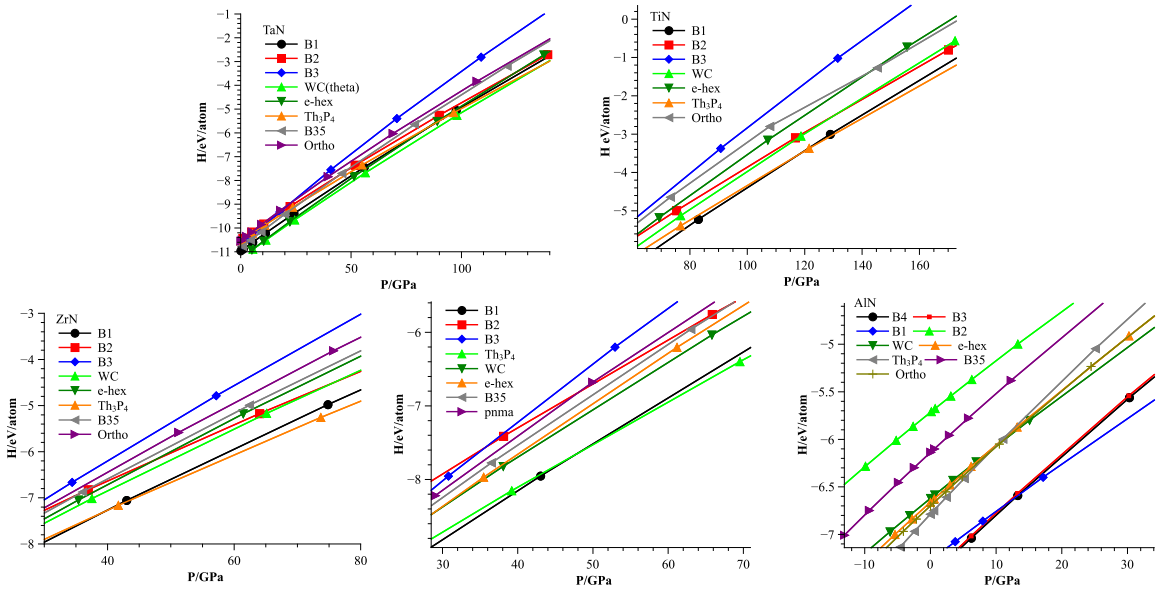

Figure 3. Enthalpy vs. Pressure behavior of the binary nitride systems

For AlN, a pressure induced phase transition to rocksalt structure (B1) can be identified, at ca. 15 GPa. Indications Experimental work reports the transition occurring between pressures values ranging from less than 14 GPa to ca. 20 GPa. We note that the value reported here excludes any influence of locally strained states due to film formation, and the effect of defects. Contrary to what other reports have shown there is no crossover in the enthalpy vs. P lines for B3 and B1 phases in AlN.

For TiN, both the B3 and WC structures lies second in stability after the B1 phase, at conditions of P=0, at higher pressures, the B35 structure lies lower in the H vs. P diagram, close to 117 GPa. For TiN the rocksalt structure is the preferred structure, for up to a very high pressure; ca. 330 GPa, where it undergoes a transformation to B2 phases. For TaN, the B2 structure is only stable at extreme pressures. We observe a phase transformation from δ-hex to B2 at 230 GPa.

4. Concluding remarks

The energetic behavior of the experimentally found phases of AlN, TiN, TaN, HfN and ZrN as obtained from first principles total energy DFT calculations are reported. In addition to the experimentally observed ambient condition phases, for exploring high pressure-phase diagrams other proposed phases are also studied. For the case of AlN, the zinc-blend and wurzite structures lie remarkably close in energy, especially below 90 GPa. This explains the experimental observation of the B3 phase found in cases in which template layers are used. Above 16 GPa, the enthalpy curve shows that most stable phases is the rocksalt structure, which, explains the observed metastable behavior. The elastics constant and bulk modulus of the all phases of AlN, TiN, TaN and HfN and ZrN explored in this study are also reported. Results for the B1-NaCl crystal structures are acceptable compared to the relevant available literature. The elastic constants for most of the crystal structures studied in this paper may provide a basis for comparison for new experimental and theoretical work on these materials.

Acknowledgements

The research here supported by ARO-MURI: Insensitive Munitions. O.U.O. acknowledges gratefully CONACYT for its kind support for earlier part of his doctoral work. The authors would like to thank the support of the Laboratory of Molecular Simulations (LMS) and the Supercomputing Center of Texas A&M University, College Station, and Texas A&M University, Qatar.

References

Bazhanov, D. I., Knizhnik, A. A., Safonov, A. A., Bagatur'yants, A. A., Stoker, M. W. & Korkin, A. A. (2005), `Structure and electronic properties of zirconium and hafnium nitrides and oxynitrides', Journal of Applied Physics 97(4), 44106-44108.

Bazhanov, D. I., Safonov, A. A., Bagatur'yants, A. A. & Korkin, A. A.(2004), `The structure and electronic properties of Zr and Hf nitrides and oxynitrides', Micro- and Nanoelectronics 2003 5401, 418-425.

Birch, F. (1947), `Finite Elastic Strain of Cubic Crystals', Physical Review 71(11), 809.

Chen, X.-J., Struzhkin, V. V., Wu, Z., Somayazulu, M., Qian, J., Kung, S., Christensen, A. N., Zhao, Y., Cohen, R. E., Mao, H.-k. & Hemley, R. J. (2005), `Hard superconducting nitrides', PNAS 102(9), 3198-3201.

Ching, W. Y. & Harmon, B. N. (1986), `Electronic Structure of AlN', Physical Review B 34(8), 5305-5308.

Christensen, N. E. (1994), `Optical and structural properties of III-V nitride structures under pressure', Physical Review B 50(7), 4397-4415.

Clayton, J. D. (2011), `A Nonlinear Thermomechanical Model of Spinel Ceramics Applied to Aluminum Oxynitride (AlON)', Journal of Applied Mechanics 78(1), 11011-11013.

Conroy, L. E. & Christensen, A. N. (1977), `Preparation and Crystal Structure of Beta-Ta2N', Journal of Solid State Chemistry 20(2), 205-207.

Ferreira da Silva, A., Souza Dantas, N., de Almeida, J. S., Ahuja, R. & Persson, C. (2005), 'Electronic and optical properties of wurtzite and zinc-blende TlN and AlN', Journal of Crystal Growth 281(1), 151–160.

Figueroa, U., Salas, O. & Oseguera, J. (2004), 'Production of AlN films: ion nitriding versus PVD coating', Thin Solid Films 469-470, 295–303.

Georg Brauer & Karl Heinz Zapp (1954), 'Die Nitride des Tantals', Zeitschrift fur Anorganische und Allgemeine Chemie 277(3-4), 129–139.

Gerstenberg, D. & Calbick, C. J. (1964), 'Effects of Nitrogen Methane + Oxygen on Structure + Electrical Properties of Thin Tantalum Films', Journal of Applied Physics 35(2), 402–407.

Gusev, A. (1997), 'Radiation Resistance of materials and nonstoichiometry', Doklady Akademil nauk 357(4), 490–494.

Hill, R. (1975), 'On the elasticity and stability of perfect crystals at finite strain', Mathematical Proceedings of the Cambridge Philosophical Society 77(01), 225–240.

Hohenberg, P. & Kohn, W. (1964), 'Inhomogeneous Electron Gas', Physical Review 136, B864.

Hu, Q., Noda, T., Tanigawa, H., Yoneoka, T. & Tanaka, S. (2002), 'The oxygen-related defect complexes in AlN under gamma irradiation and quantum chemistry calculation', Nuclear Instruments and Methods in Physics Research Section B: Beam Interactions with Materials and Atoms 191(1-4), 536–539.

Jeffrey, G. A. & Wu, V. Y. (1963), 'The structure of aluminum carbonitrides', Acta Crystallographica 16, 559–566.

Kang, C. S., Cho, H. J., Kim, Y. H., Choi, R., Onishi, K., Shahriar, A. & Lee, J. C. (2003), 'Characterization of resistivity and work function of sputtered-TaN film for gate electrode applications', Journal of Vacuum Science & Technology B: Microelectronics and Nanometer Structures 21(5), 2026–2028.

Kohn, W. & Sham, L. J. (1965), 'Self-Consistent Equations Including Ex- change and Correlation Effects', Physical Review 140(4A), A1133.

Kresse, G. & Furthmuller, J. (1996a), 'Efficiency of ab-initio total energy calculations for metals and semiconductors using a plane-wave basis set', Computational Materials Science 6(1), 15–50.

Kresse, G. & Furthmuller, J. (1996b), 'Efficient iterative schemes for ab initio total-energy calculations using a plane-wave basis set', Physical Review B 54(16), 11169.

Kresse, G. & Hafner, J. (1993), 'Ab initio molecular dynamics for liquid metals', Physical Review B 47(1), 558.

Kresse, G. & Joubert, J. (1999), 'From utrasoft pseudopotentials to the projector augmented wave method', Physical Review B 59, 1758.
Lambrecht, W. R. L., Miao, M. S. & Lukashev, P. (2005), 'Magnetic properties of transition-metal nitrides', 49th Annual Conference on Magnetism and Magnetic Materials 97, 10D306–3.
Levy, F., Hones, P., Schmid, P. E., Sanjines, R., Diserens, M. & Wiemer, C. (1999), 'Electronic states and mechanical properties in transition metal nitrides', Surface and Coatings Technology 120-121, 284–290.
Lopez, G. & Staia, M. H. (2005), 'High-temperature tribological character- ization of zirconium nitride coatings', Surface and Coatings Technology 200(7), 2092–2099.
M. Lerch, E. F. J. W. (1996), 'Synthesis, Crystal Structure, and High Tem- perature Behavior of Zr3N4', Zeitschrift fur Anorganische und Allgemeine Chemie 622(2), 367–372.
Mashimo, T., Tashiro, S., Nishida, M., Miyahara, K. & Eto, E. (1997), 'B1- type and WC-type phase bulk bodies of tantalum nitride prepared by shock and static compressions', Physica B: Condensed Matter 239(1-2), 13–15.
Mehl, M. J. (1993), 'Pressure dependence of the elastic moduli in aluminum- rich Al-Li compounds', Physical Review B 47(5), 2493.
Meng (1994), 'Crystal structure, mechanical properties, thermal properties and refractive index of AlN', Properties of group III Nitrides.
Merad, A. E., Kanoun, M. B., Cibert, J., Aourag, H. & Merad, G. (2003), 'Ab initio study of electronic properties of zincblende AlN and deformation potentials under hydrostatic stress', Materials Chemistry and Physics 82(2), 471–477.
Nye, J. F. (1985), 'Physical Properties of Crystals: Their Representation by Tensors and Matrices '.
Ojeda Mota, O. & Cagın, T. (2011), 'Anisotropic behavior of energetic materials at elevated pressure and temperature', Journal of Loss Prevention in the Process Industries 24, 805-13.
Petrunin, V. F. & Sorokin, N. I. (1982), 'Structure and Stability of Tantalum Nitrides', Inorganic Materials 18(12), 1733–1736.
Pierson, H. O. (1996), 'Handbook of Refractory Carbides and Nitrides'.
Pugh, S. K., Dugdale, D. J., Brand, S. & Abram, R. A. (1999), 'Electronic structure calculations on nitride semiconductors', Semiconductor Science and Technology (1), 23.
Rivadulla, F., Banobre Lopez, M., Quintela, C. X., Pineiro, A., Pardo, V., Baldomir, D., Lopez-Quintela, M. A., Rivas, J., Ramos, C. A., Salva, H., Zhou, J.-S. & Goodenough, J. B. (2009), 'Reduction of the bulk modulus at high pressure in CrN.', Nature Materials 8(12), 947–951.
Schulz, H. & Thiemann, K. H. (1977), 'Crystal structure refinment of AlN and GaN', Solid State Communications 23, 815–819.
Sedmidubsky, D. & Leitner, J. (2006), 'Calculation of the thermodynamic properties of AIII nitrides', Journal of Crystal Growth 286(1), 66–70.
Song, D. Y., Holtz, M., Chandolu, A., Nikishin, S. A., Mokhov, E. N., Makarov, Y. & Helava, H. (2006), 'Optical phonon decay in aluminum nitride', Applied Physics Letters 89, 21901–21903.
Stampfl, C., Mannstadt, W., Asahi, R. & Freeman, A. J. (2001), 'Elec- tronic structure and physical properties of early transition metal mononi- trides: Density-functional theory LDA, GGA, and screened-exchange LDA FLAPW calculations', Physical Review B 63(15), 155106.
Stejskal, J. & Leitner, K. (2002), 'Aluminum, gallium and indium nitrides - advanced materials in electronics', Chemicke Listy 5(96), 311–320.
Storms, E. K. (1964), 'A critical review of refractories'.
Terao, N. (1971), 'Structure of Tantalum Nitrides', Japanese Journal of Applied Physics 10(2), 248–259.
Tsvyashchenko, A. V., Popova, S. V. & Alekseev, E. S. (1980), 'Band Structure of Hexagonal Tantalum Nitride', physica status solidi (b) 100(1), 99– 102.
Wallace, D. C. (1972), Thermodynamics of Crystals, Dover, New York.
Werner H. Baur, M. L. (1996), 'On Deciding between Space Groups Pnam and Pna21 for the Crystal Structure of Zr3N4', Zeitschrift fur Anorganis- che und Allgemeine Chemie 622(10), 1729–1730.
Wright, A. F. (1995), 'Consistent structural properties for AlN, GaN, and InN', Physical Review B 51(12), 7866–7869.
Wu, Z., Chen, X.-J., Struzhkin, V. V. & Cohen, R. E. (2005), 'Trends in elasticity and electronic structure of transition-metal nitrides and carbides from first principles', Physical Review B 71(21), 214103.
Zaoui, A. (2003), 'Plane wave pseudopotential study of ground state properties and electrochemical description of thallium nitride', Materials Sci- ence and Engineering B: Solid-State Materials for Advanced Technology 103(3), 258–261.
Zerr, A., Miehe, G. & Riedel, R. (2003), 'Synthesis of cubic zirconium and hafnium nitride having Th3P4 structure', Nature Materials 2(3), 185–189.
Zerr, Andreas, Gerhard Miehe, Jinwang Li, Dmytro A. Dzivenko, Vadim K. Bulatov, Heidi Hofer, Nathalie Bolfan-Casanova, Michel Fialin, Gerhard Brey, Tomoaki Watanabe & Masahiro Yoshimura (2009), 'High-Pressure Synthesis of Tantalum Nitride Having Orthorhombic U2S3 Structure', Advanced Functional Materials 19(14), 2282–2288.